Nuclear Inst. and Methods in Physics Research, A 1015 (2021) 165762

Contents lists available at ScienceDirect

Nuclear Inst. and Methods in Physics Research, A

journal homepage: www.elsevier.com/locate/nima

# Multipurpose Ce-doped Ba-Gd silica glass scintillator for radiation measurements

V. Dormenev [a,*], A. Amelina [b,c], E. Auffray [d], K.-T. Brinkmann [a], G. Dosovitskiy [b,c], F. Cova [e], A. Fedorov [b], S. Gundacker [d], D. Kazlou [f], M. Korjik [b,f], N. Kratochwil [d,g], V. Ladygin [h], V. Mechinsky [b,f], M. Moritz [a], S. Nargelas [i], R.W. Novotny [a], P. Orsich [a,f], M. Salomoni [d], Y. Talochka [f,i], G. Tamulaitis [i], A. Vaitkevicius [i], A. Vedda [e], H.-G. Zaunick [a]

[a] 2nd Physics Institute, Justus-Liebig-University, Heinrich-Buff-Ring 16, 35392 Giessen, Germany
[b] NRC "Kurchatov Institute", 1 Kurchatov sq., Moscow, Russia
[c] NRC "Kurchatov Institute"-IREA, 3 Bogorodskiy val, Moscow, Russia
[d] CERN, Route de Meyrin, 1211 Geneva 23, Switzerland
[e] Department of Materials Science, University of Milano - Bicocca, Via Cozzi 55, 20125 Milano, Italy
[f] Institute for Nuclear Problems of Belarus State University, Bobruiskaya 11, 220030 Minsk, Belarus
[g] University of Vienna, Universitaetsring 1, 1010 Vienna, Austria
[h] Joint Institute for Nuclear Research, Moscow region, 141980, Dubna, Russia
[i] Institute of Photonics and Nanotechnology, Vilnius University, Sauletekio al. 3, LT-10257 Vilnius, Lithuania

ARTICLE INFO

*Keywords:*
Scintillator
Glass
Ionizing radiation
Detectors

ABSTRACT

A new inorganic scintillation material based on Ba-Gd silica glass doped with cerium (BGS) is fabricated and studied. With the highest light yield among heavy glasses at the level of 2500 ph/MeV and fast scintillation response, the new scintillator ensures a good coincidence time resolution of < 230 ps FWHM for 511 keV $\gamma$-quanta from a $^{22}$Na source and SiPM readout. In addition to good performance in $\gamma$-quanta detection, the material demonstrates capability for efficient detection of low-energetic neutrons. The scintillator is produced by exploiting the standard industrial glass technology, which allows for an unlimited scaling up the conversion of raw material into a high-quality scintillator at a high rate. The glass can be casted in application-specific molds, so minimizing the material losses. The presented glass scintillator has potential for further improvement of its light output and scintillation response time.

## 1. Introduction

Oxide glasses and glass ceramics made from binary compounds and containing metal and silica oxides have been found to be a good matrix to develop scintillation materials doped with Ce ions [1]. Silica glasses produced by sol–gel method and doped with Ce or Pr were found to be promising scintillation materials for medical and high energy physics (HEP) applications [2–4]. Other light glasses, with a relatively high light yield, which, however, is a few times smaller than the typical light yields of single-crystal scintillation materials [5–7], are Li-based compounds. Nevertheless, they are successfully used to detect thermal neutrons when the glass is enriched with $^{6}$Li ions. In contrast, the enrichment of the glass with $^{7}$Li ions makes it insensitive to thermal neutrons. Moreover, there are ongoing attempts in replacing Pb by Bi to trigger a new turn of the development of heavy and possibly scintillating glass for the needs in HEP applications.

The glass based on barium di-silicate BaO-2SiO$_2$ (DSB) might become a new scintillation material suitable for operation even in harsh radiation environments such as those in collider experiments [8–11]. This glass is produced from an inexpensive initial charge and allows manufacturing in large quantities by standard technology exploited in the glass industry. It exhibits relatively fast response; its light yield is lower than that of the most efficient scintillators but exceeds the light yield of PbWO$_4$, which is nowadays the most extensively used scintillating material in HEP experiments [12]. However, the radiation length is by far not compatible and could be considered for a sampling calorimeter concept only. The initial DSB composition can be supplemented by loading with rare-earth oxides and the corresponding amount of silica oxide. As a result, the light yield of the glass can reach up to 30% of that in the well-known scintillator BGO [13]. In parallel, the density can be increased to 4.2 g/cm$^3$ or even higher, which enhances capabilities of detecting low-energy gamma quanta below 1 MeV with acceptable energy resolution and designing heterogeneous detection cells of "shashlik" or "spaghetti " type. Furthermore, the enrichment of barium-silica glass with gadolinium is preferable, because Gd oxide

* Corresponding author.
*E-mail address:* valery.dormenev@exp2.physik.uni-giessen.de (V. Dormenev).

https://doi.org/10.1016/j.nima.2021.165762
Received 30 January 2021; Received in revised form 20 August 2021; Accepted 21 August 2021
Available online 24 August 2021

is by a factor of ten less expensive than Lu oxide. Moreover, in contrast to Lu, natural gadolinium does not contain radioactive isotopes.

Besides the use in detector technology for $\gamma$-detection, for which the material may be manufactured in various shapes at low cost, the relatively fast scintillation and sufficient light yield of Ba-Gd silica glass doped with cerium (BGS) could become attractive also for industrial introscopy or neutron detection, provided that the slow components could be significantly reduced for high-rate applications. Recently, we demonstrated that Gd-based inorganic scintillation materials are in general suitable to detect neutrons in a wide energy range [14]. First results on the BGS glass scintillator response to neutrons are reported here. The improvements of the new material achieved with the support of the ATTRACT-SCINTIGLASS project [15] are reported as well.

## 2. Production technology of Ba-Gd silica glass

The production of initial DSB:Ce glass samples of different qualities, compositions, and shapes was performed in order to study their basic scintillation performance [8,10,13,16,17]. The achieved luminescence parameters as well as the radiation hardness have been very promising. The first samples of large volume of up to 20x20x100 $mm^3$ have been assembled into a 3x3 matrix read out using photomultiplier tubes to measure the response to high energy photons of up to 100 MeV [18]. However, the achievable response was limited in most of the samples by inhomogeneous optical transparency due to bubbles in the glass matrix. These imperfections were caused by technical limitations of the available ovens.

The SCINTIGLASS project provided the opportunity to start a joint development of academy researchers with the internationally well-known and experienced glass manufacturer Preciosa (Czech Republic). For technical reasons, the project was focused on the development of BGS glass leading to a significant improvement of the initial material.

$BaCO_3$, $CeO_2$, $Gd_2O_3$, and $SiO_2$ of analytical grade were used as starting materials. The glasses were synthesized by melt-quenching technique. The chemicals were mixed in an appropriate proportion and homogenized by milling. The glass was melted in corundum crucibles of 50–500 ml volume for 2 h in a furnace with resistive heating under atmospheric conditions. The synthesis temperature was 1550 °C. The amount of Ce oxide in the initial mixture was chosen to be in the range from 0.3 to 1.5 weight %. The molten glass was casted in a mold and the obtained samples were annealed at 700 °C for 4 h in a muffle furnace to reduce stress before mechanical treatment. The progress in the glass quality is illustrated in Fig. 1 showing the changing color of the obtained glass bulks with dimensions not less than 25x25x100 $mm^3$. After the first experimental phase of 8 months since the start of the development, colorless bulks were obtained. Technological efforts were aimed at obtaining a heavy scintillation glass combining an improved light yield and faster scintillation kinetics with respect to those of the previous generation material.

An additional set of glass elements was produced at NRC "Kurchatov Institute"-IREA. The plates were produced by casting in a mold to produce scintillation elements with dimensions of 40x40x5 $mm^3$ for the prototype of a special calorimetric module of the SPD experiment at the NICA Collider (JINR, Dubna) [19].

## 3. Characterization techniques

Optical and scintillation properties of colorless glass samples have been evaluated by different spectroscopic techniques.

X-ray excited radio-luminescence (RL) and thermally-stimulated luminescence (TSL) measurements were carried out with a custom-made apparatus featuring a CCD detector (Jobin-Yvon Syncerity) equipped with a 234 grooves/mm grating. RL was excited by X-ray irradiation using a Philips PW2274 tube operating at 20 kV. The TSL measurements were performed by irradiating at a dose rate of approximately 0.2 Gy/s; the accumulated dose was ~180 Gy. A heating rate of 0.1 K/s was adopted and the TSL signal was collected using a sampling of 5 K. Measurements were performed in the temperature range between 10 K and 320 K. The sample was glued to the cold finger of the cryostat by means of Ag paint in order to achieve a good thermal contact. The emission spectra have been corrected for the spectral response of the detection system. By integrating within the emission wavelength range (340–600 nm), the TSL intensity as a function of temperature was obtained (hereafter called "glow curve").

TSL measurements above RT up to 700 K have been recorded at a heating rate of 1 K/s and a sampling of 3 K. The acquisition system was based on a nitrogen-cooled CCD detector coupled to a monochromator (Jobin-Yvon MicroHR) equipped with a 150 grooves/mm grating. The X-ray irradiation was operated using a Machlett OEG50 X-ray tube with W anode operated at 20 kV (dose rate 0.5 Gy/s); the cumulated delivered dose was about 165 Gy.

For optical absorption, the spectrophotometers Varian Cary 50 or 4000 were used. The optical absorption spectra were acquired between 190 nm and 1100 nm. The population of the emitting level of $Ce^{3+}$ ions and the decay of electronic excitation were studied by the transient absorption technique (see [14] for details). The output of a Yb:KGW laser emitting 200 fs-long pulses was split into two beams. The pump beam was equipped with harmonics generators and a parametric amplifier to tune the energy of excitation photons. The transient absorption (TA) due to the pump-pulse-excited non-equilibrium electrons was probed by pulses of white continuum light in the range from 1.3 eV to 2.7 eV (950–460 nm) generated by the second beam and focused on the excited spot of the studied crystal. The optomechanical delay line on the path of the probe beam enabled measuring the transient absorption at different delays between pump and probe pulses. The TA spectra have been recorded as the difference in the optical absorption with and without pump-pulse excitation. The measurements have been repeated at different delays between the pump and probe pulses.

Scintillation kinetics was measured by standard start/stop technique [20,21]. The scintillation light has been detected using a 2-inch Hamamatsu R2059-01 photomultiplier tube (PMT) with bialkali photocathode with 21 % quantum efficiency at the scintillator emission peak (430 nm). All measurements have been performed at room temperature in a box with the temperature stabilized within ±0.5°C. The anode output of the PMT was digitized in a charge sensitive Analogue-to-Digital Converter (ADC) with variable integration gates. The response to low-energy $\gamma$-rays of a $^{137}Cs$ source has been calibrated using the single-electron signal. The light yield measurements were performed in the range of temperatures between −40 °C and +20 °C The irradiation facility at the Justus Liebig University exposing the samples to $\gamma$-rays of $^{60}Co$ with a typical dose rate of 1 Gy/minute was utilized to evaluate the material tolerance to ionizing radiation.

The subset of samples produced at the Kurchatov Institute has been tested in a similar manner using a low-energy $^{137}Cs$ source. The scintillation light has been detected with a commercial Phillips photomultiplier XP2020 (QE ≈ 20%). The absolute light yield has been determined by comparison to the response of a calibrated reference glass sample GS-20 (Saint-Gobain).

Coincidence time resolution (CTR) measurements were performed at room temperature using 2x2x3 $mm^3$ samples coupled to Hamamatsu Si-Photomultipliers (SiPM) (HPK S13360 3050PE) having a photodetection efficiency of ~60% at 430 nm and an intrinsic single-photon time resolution (SPTR) of 135 ± 8 ps FWHM [22], a $^{22}Na$ source, and electronics described elsewhere [23].

A standard Am-Be source (ISO 8529-1: 2001 (E)) at the Radiation Center of Justus-Liebig University (Giessen, Germany) was used to measure the response to neutrons. The activity of the $^{241}Am$ source was 220 GBq, the calculated neutron yield in $4\pi$ geometry $1.3 \times 10^7$ n/s, and the peak of the neutron energy distribution was at ~4 MeV. A BGS sample with dimensions of 20x20x5 $mm^3$ coupled to a Hamamatsu R2059-01 photomultiplier was placed in the neutron source in a well with a diameter of 80 mm. Combinations of additional materials for

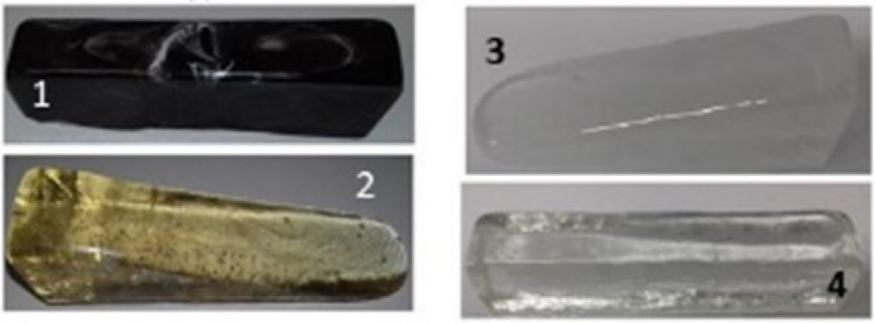


**Fig. 1.** Typical BGS:Ce glass bulks produced as the first attempt (1) and two (2), five (3) and eight months (4) after starting the development on industrial facilities.

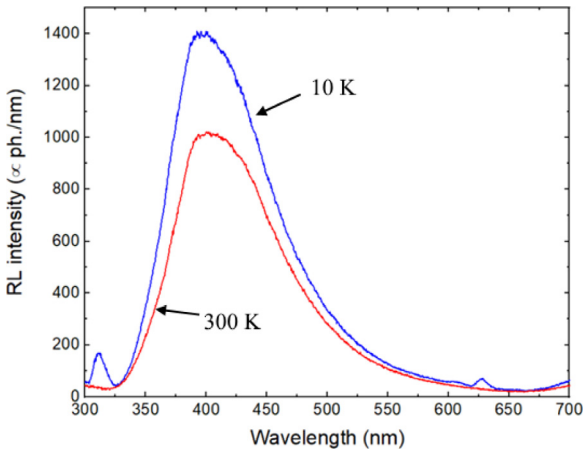


**Fig. 2.** Cerium-doped BGS glass radio-luminescence spectra at 300 and 10 K. The sample has 0.76 weight % of $Ce_2O_3$ in initial charge.

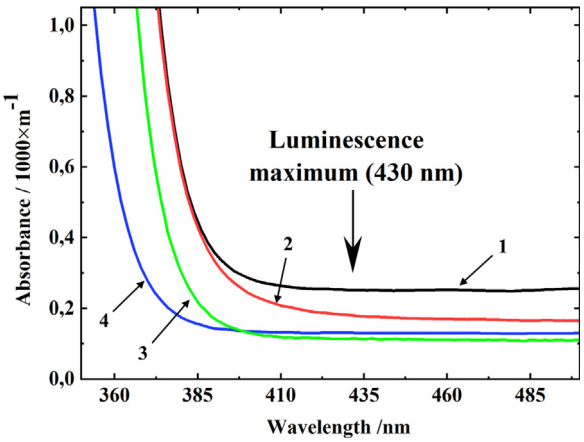


**Fig. 3.** Absorption spectra at the absorption edge of Ce-doped BGS glasses produced at different development stages and with different Ce-content (in $Ce_2O_3$ weight % in the initial charge): 0.3 weight % at the beginning of the project (1), 0.76 weight % (2) and 1.1 weight % (3) produced by PRECIOSA 8 months after project start, and 1.17 weight % produced prior the project (4). Samples produced prior to the project show stronger light scattering.. (For interpretation of the references to color in this figure legend, the reader is referred to the web version of this article.)

moderation or absorption were placed between the neutron source and the detector. Discs of 80 mm in diameter made of lead and copper with thicknesses of 14 to 40 mm and 3 mm, respectively, were used to suppress the accompanying gamma radiation from the Am-Be neutron source, in particular the 4.44 MeV line, as well as the fraction of the natural gamma background. Copper was used to absorb the characteristic X-ray radiation of lead. A 10 cm-thick polyoxymethylene cylinder was used to moderate the neutron flux from the source. A 2 mm-thick cadmium filter absorbed the thermal neutrons.

## 4. General characterization of Ce-doped BGS glasses

The RL spectra of the studied samples are shown in Fig. 2. In a wide temperature range, the spectra consist of a band peaking at 430 nm due to the transitions 5d $\rightarrow {}^2F_{5/2,7/2}$ in $Ce^{3+}$. An additional emission band peaking at 313 nm is observed beside the main Ce emission band at low temperatures (see the spectrum at 10 K in Fig. 2). This band is attributed to $P_6$-$S_8$ *f-f* electronic transition of $Gd^{3+}$. The quenching of $Gd^{3+}$ luminescence at room temperature confirms an efficient transfer of the electronic excitations from $Gd^{3+}$ subsystem to $Ce^{3+}$ ions. The Gd ions in the glass enhance the Coulomb-interaction-driven transfer of excitation to $Ce^{3+}$ ions playing the same role for the increase of the light yield as observed in Gd-based crystalline materials [24].

After the first developments of DSB-type scintillation glasses [8–10], a substantial progress in the light yield has recently been achieved due to better understanding of the scintillation mechanism in Ce-doped glasses [2–4,25,26]. The poor efficiency of excitation transfer to the activator $Ce^{3+}$ ions in a disordered glass matrix can be improved by an increase in activator content in the glass. Fig. 3 shows the variation of the optical absorption edge of BGS glasses grown at different technology development stages from the initial charge containing different concentrations of Ce. The absorption edge in the absorption spectrum of the last samples optimized for the preproduction phase (blue and green curves in Fig. 3) is blue shifted in respect to that of the first small samples (black and red curves) containing a substantially larger concentration of $Ce^{3+}$ ions. Note that only minor absorption in the spectral range of the scintillation light is observed in the optimized samples.

At high Ce content in the glass, a part of Ce ions inherently exists in the $Ce^{4+}$ state and may result in a brownish coloration of the glass due to a wide and structureless $Ce^{4+}$-related absorption band extending from the visible to UV range. The presence of $Ce^{4+}$ in the glass results in a drop of the scintillation light yield due to reabsorption. To prevent this effect, the prevalence of cerium ions in $Ce^{3+}$ valence state in the glass can be facilitated by adding special ingredients to the glass composition before melting. For instance, adding SiC allows one to keep reducing conditions inside the oven when operating in a specific gas or even natural atmosphere [1]. Fig. 4 presents the correlation between the optical transmission at 390 nm, where the absorption $Ce^{4+}$ dominates and $Ce^{3+}$ absorption is insignificant, and the light yield for all samples produced by Preciosa in the course of the project. The strong correlation evidences a strong influence of the activator in $Ce^{4+}$ state.

A comparison of photoluminescence and scintillation kinetics in Ce-doped BGS glass measured at room temperature by the start/stop method is presented in Fig. 5. The photoluminescence exhibits a single exponential decay with a time constant of 50 ns. Meanwhile, the scintillation decay proceeds at a substantially slower rate. The decay can

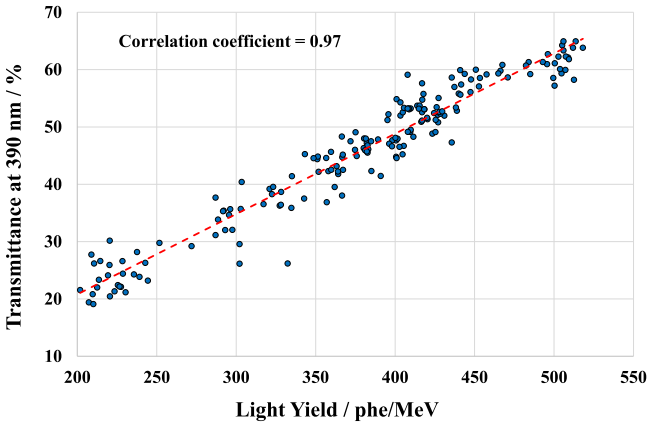


**Fig. 4.** Correlation between the optical transmission of 5 mm-thick glass samples at a wavelength of 390 nm and the light yield measured at room temperature using a PMT with bialkali photocathode. Samples have been produced at the pre-production run with 0.76 weight % of $Ce_2O_3$.

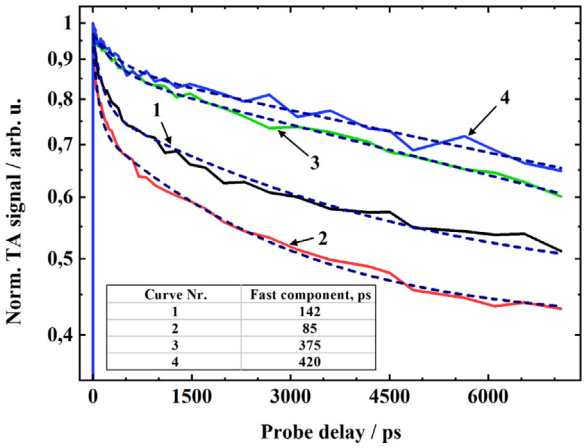


**Fig. 6.** Transient absorption kinetics probed at photon energy of 2.15 eV in Ce-doped BGS glasses (the same glasses as in Fig. 3) produced at different development stages and with different Ce-content (in $Ce_2O_3$ weight % in the initial charge): 0.3 weight % at the beginning of the project (1), 0.76 weight % (2) and 1.1 weight % (3) produced by PRECIOSA 8 months after project start, and 1.17 weight % produced prior the project (4). Dashed curves correspond to biexponential fit of the decay. The decay time of the slow component is ~22 ns for all the samples and the fast is indicated in the figure.

be described by two components with comparable contributions: fast component with time constant of 90 ns (45%) and s slow component with time constant of 400 ns (55%).

In order to clarify the scintillation kinetics, the electronic excitation transfer processes have been investigated by studying the transient absorption (TA) from the radiative state of $Ce^{3+}$, as in [14]. The kinetics of the TA signal probing the population of radiative state of $Ce^{3+}$ ions in the glass have been performed after selective excitation of the second excited state of $Ce^{3+}$ with 3.75 eV (330 nm) pump photons. The results for a few typical samples are shown in Fig. 6. The rising part of the kinetics is in sub-picosecond domain and follows the excitation pulse, whereas the decay part contains two components. The decay time of the fast component correlates with the Ce concentration in the glass: it becomes shorter for larger $Ce^{3+}$ content. Nevertheless, its fraction in the total TA signal is small relative to that of the second component with a time constant of ~22 ns, which is similar for all samples. Note that the TA signal reflects the population of the emitting level of $Ce^{3+}$ defining the luminescence intensity, however, the TA kinetics is measured within the initial stage of population of the emitting level, which is shorter than the time resolution of the luminescence measurements presented in Fig. 5.

Fig. 7 shows the results of TSL measurements. Only the $Ce^{3+}$ luminescence is observed in the contour plots of the TSL signal. Below room temperature a broad TSL structure is observed, as expected for an amorphous material: it peaks at 240 K.

The decreasing signal at very low temperatures might be attributed to an athermal tunneling recombination mechanism but deserves further investigation. Above room temperature, a wide and asymmetric band peaked at ~350 K is observed. The signal above 600 K (not displayed) is dominated by the black body radiation. The TSL peaks indicate the presence of electron traps in the glass; their origin is still unknown, but their depletion near room temperature, which is a quite typical scintillator operation temperature, indicates a possible influence of the traps on excitation transfer processes in the glass, for example giving rise to slow decay components. The minimization of the influence of the traps on the scintillation properties of Ce-doped BGS glasses is a matter of forthcoming efforts.

Fig. 8 demonstrates the time delay distribution between two channels obtained in CTR measurements with 511 keV $\gamma$-quanta from a $^{22}Na$ source and SiPM readout at room temperature. The CTR FWHM was found to be 215 ps exploiting both scintillation and Cherenkov emission. This result is only by a factor of 3.5 longer than the CTR obtained in the same conditions with the same pixel size of LSO material extensively used in PET scanners [22]. In further tests to adjust the time walk correction using different rise time windows between the single signal amplitude of the first and second photon detected (50 mV–120 mV) and after correction, a good time resolution of FWHM = 163 ± 8 ps for all photoelectric events has been achieved. Similar to [27], using only the fastest third of the events per channel (11% of the events in coincidence) leads to a time resolution of FWHM = 100 ± 6 ps (see Fig. 9). The structures in the distribution are not significant within the error bars. This concept of time walk correction

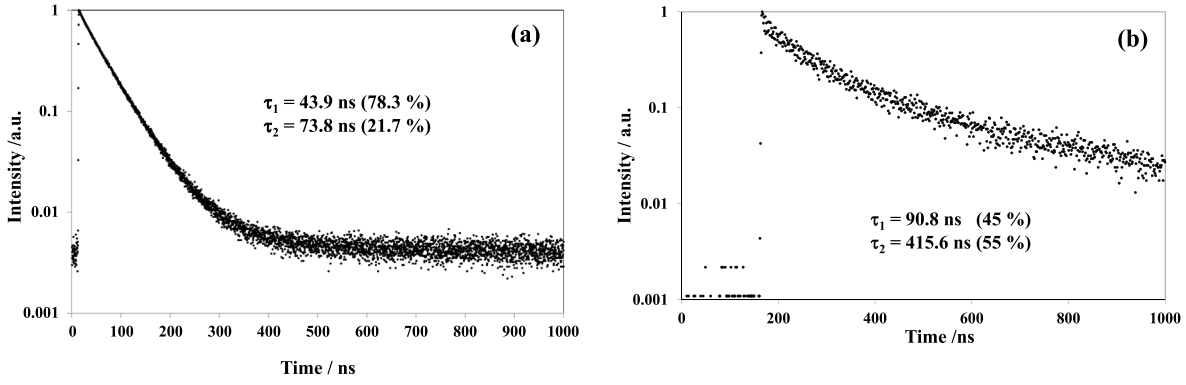


**Fig. 5.** Kinetics of photoluminescence ($\lambda_{ex}$ = 360 nm) (a) and scintillation kinetics (b) of a typical BGS scintillation glass fabricated with $CeO_2$ concentration of 0.7 weight % in the initial charge.

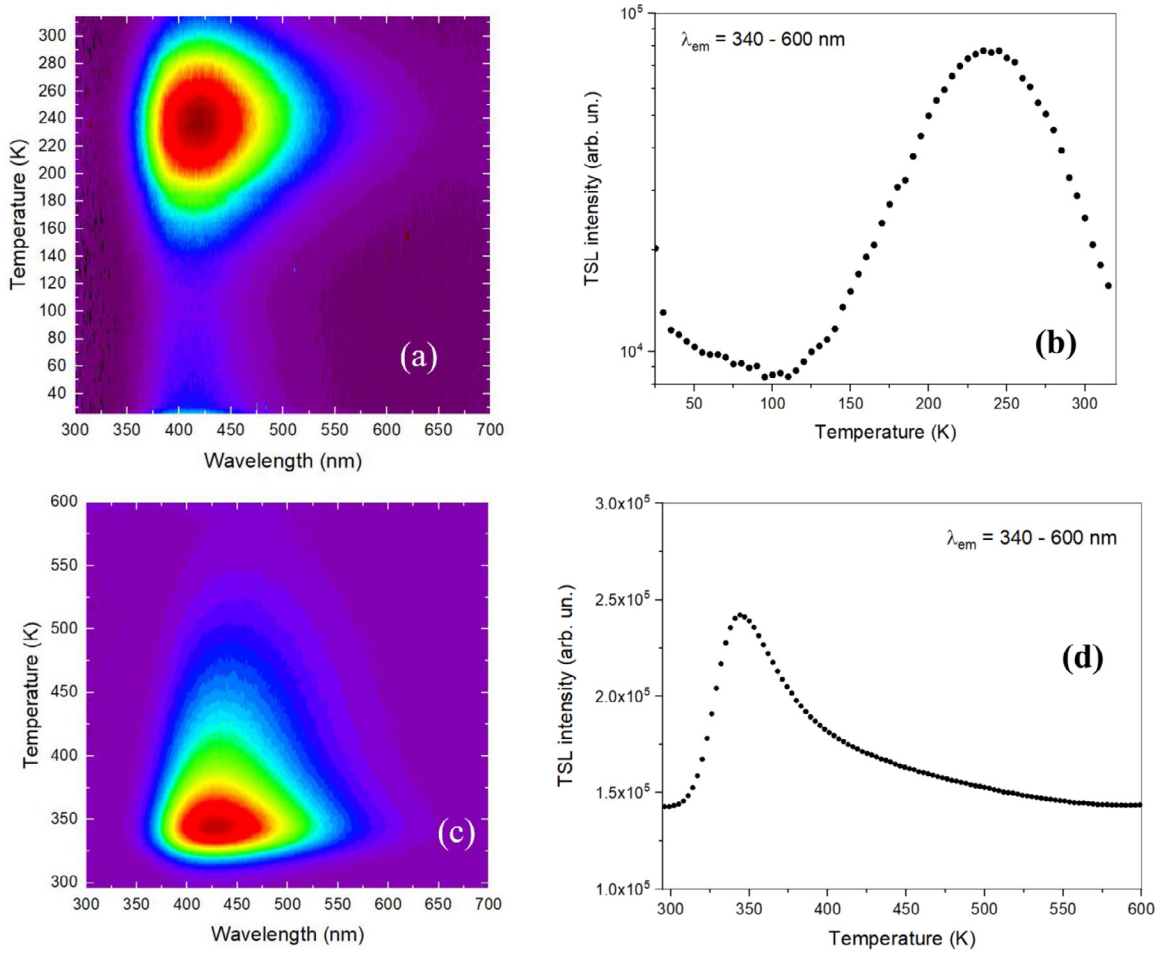


**Fig. 7.** Thermally stimulated luminescence contour plots (a, c) and the related glow curves (b, d) obtained by integrating luminescence intensity in the wavelength range of Ce emission (340–600 nm)..

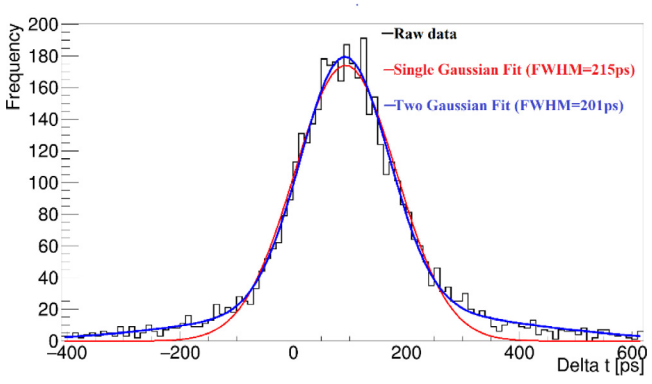


**Fig. 8.** Time delay distribution between two identical DSB samples at CTR measurement acquired with 511 keV $\gamma$-quanta from a $^{22}$Na source and SiPM readout at room temperature and 10 mV leading edge threshold. Raw data were fitted with a single Gaussian fit function and with a sum of two Gaussian fit functions, as described in [27].

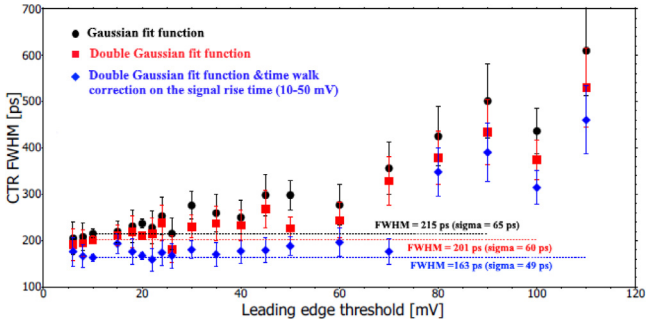


**Fig. 9.** Coincident time resolution as a function of leading-edge threshold for different steps of analysis.

and exploiting Cherenkov emission are fairly new and might enable further optimization of the CTR resolution.

## 5. Characterization of industrial pre-production run of Ce-doped Ba-Gd silica glass samples

Supported by the ATTRACT-SCINTIGLASS project, the first large set of Ce-doped BGS glass scintillator plates have been produced as a result of a close feedback between industrial manufacturer PRECIOSA and the teams responsible for characterization. The complete final production delivered 16 bulks with overall dimensions of 20x20x100 mm$^3$. For characterization, rectangular 17x20x5 mm$^3$ plates have been cut from the bulks, delivered in batches and labeled with ID numbers. The plate surfaces, except of two smallest side surfaces, were polished to optical quality and prepared for quality tests and later use in the first prototype of a sampling calorimeter module. In total, 183 plates of identical geometry have been fabricated and studied.

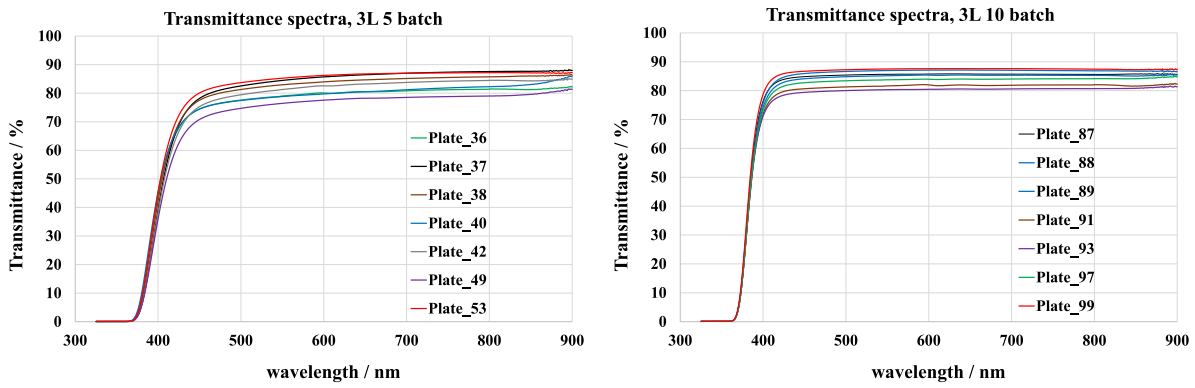


**Fig. 10.** Optical transmittance of BGS samples cut from glass blocks of two selected batches. The transmission is measured across the thickness of 5 mm.

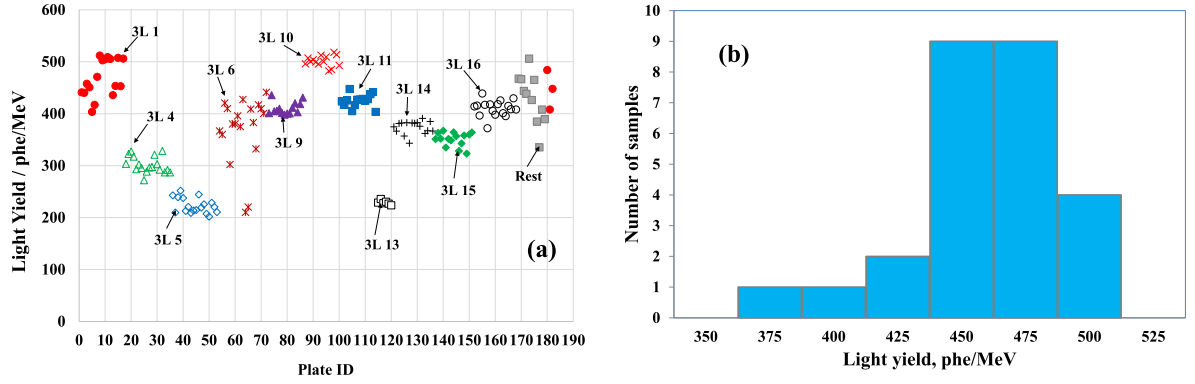


**Fig. 11.** Scintillation light yield measured at room temperature with an integration gate of 4 μs in 183 Preciosa samples grouped in batches (indicated) fabricated from the same production bulk (a) and distribution of the light yield of 40x40x5 mm scintillation selected samples with no visual coloring by NRC Kurchatov Institute (b).. (For interpretation of the references to color in this figure legend, the reader is referred to the web version of this article.)

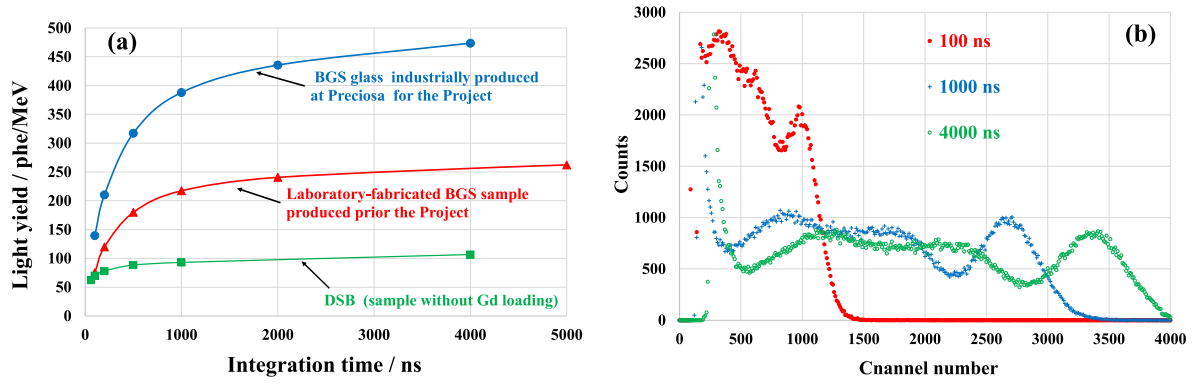


**Fig. 12.** Light yield as a function of integration gate width for three types of glass samples (a) and the response function to $\gamma$-ray excitation by a $^{137}$Cs source at different integration gates (indicated) for a typical Ce-doped BGS sample fabricated on the preproduction stage (b). All the results are obtained at room temperature.

### 5.1. Optical transmittance

Fig. 10 shows the spread of the transmission spectra of all plates cut from two selected bulks labeled 3L5 and 3L10. The transmission spectra correlate with low and high yield of scintillation light (see also Fig. 4).

### 5.2. Scintillation light yield

Fig. 11(a) summarizes the light yield of all 183 plates fabricated in the preproduction run and grouped according to the parent blocks as they have been casted. The results are given in detected photoelectrons as defined in the previous chapter 3 for an integration gate of 4 μs measured at room temperature. The variation of the light yield within any bulk is relatively small and evidences the homogeneity of the casted blocks. However, as already mentioned, the variation of the light yield from block to block increases up to a factor of two and is well correlated with the shape of the optical transmission edge. Fig. 11(b) shows for comparison the distribution of the light yield of the subset of slightly larger samples manufactured at Kurchatov Institute and characterized in Minsk. The average value and distribution are quite similar.

The response of BGS to 662 keV $\gamma$-rays is shown in Fig. 12. The light yield (see Fig. 12(a)) increases substantially as the integration gate width increases up to ~500 ns and reaches saturation beyond ~4 μs. Moreover, Fig. 12(a) evidences an impressive improvement of the light yield in glasses loaded with Gd, both in the samples fabricated in laboratory and using industrial facilities. Fig. 12(b) shows the response

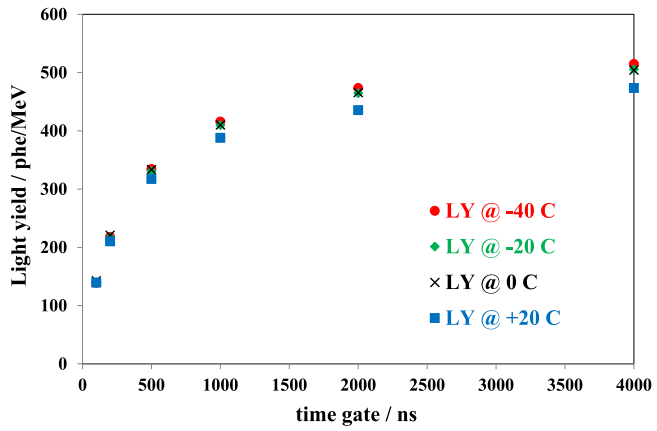


**Fig. 13.** Light yield as a function of integration gate width at different temperatures (indicated) for a typical sample # 17 selected out of the 183 delivered plates.

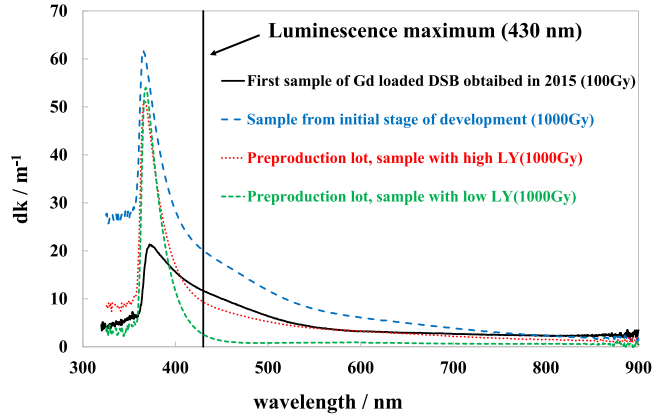


**Fig. 14.** Spectra of radiation-induced absorption coefficient after $\gamma$-irradiation for typical samples produced at different stages of technology development.

function to 662 keV $\gamma$-rays of a $^{137}$Cs source for integration gate widths of 100 ns, 1 μs and 4 μs.

The dependence of the scintillator response on the operating temperature is important for many applications. Fig. 13 shows the variation of the light yield as a function of the integration gate at a few temperatures within a wide range from −40° C to +20° C. The temperature dependence of the light yield at 4 μs integration time was measured to be below 0.3%/°C over the entire temperature range studied.

### *5.3. Tolerance to ionizing radiation and stimulated recovery of optical transmission*

Initial studies of DSB indicated sufficient tolerance of the scintillating glass to ionizing radiation: in most of the studies, samples without Gd-loading have been examined and the damage imposed by $\gamma$-rays of a high intensity $^{60}$Co source and protons with energy of even up to several GeV delivered at KVI (The Netherlands) and at CERN have been investigated [8].

Fig. 14 shows the spectrum of the radiation-induced absorption coefficient d*k* measured for first Gd loaded DSB sample and samples obtained at different stages of ATTRACT-SCINTIGLASS project after their exposure to an integral dose of up to 1 kGy. The *dk* value is defined as:

$$dk = [ln(\frac{T_b}{T_a})]/d, \quad (1)$$

where $T_b$, $T_a$ are the optical transmittances before and after irradiation, respectively, and $d$ is the sample thickness.

It has recently been shown that the radiation damage caused by electromagnetic probes in lead tungstate scintillating crystals can be effectively restored by external illumination in a wide wavelength range even down to the near infrared region [28,29]. The stimulated recovery allows reducing the transmission losses even at low temperatures when spontaneous recovery processes are substantially reduced. In addition, the restoring can be performed *in situ* by installing small light sources into the detector units. As shown in Figs. 15 and 16, a similar mechanism can be exploited for BGS glass. Two plates of relatively low (plate number #65) and high (#180) light yield have been illuminated with LEDs emitting at a wavelength of 464 nm and with intensity about $10^{16}$ photons/s. The figures show the reduction of the radiation-induced absorption coefficient as a function of time of illumination by the external light source. Significant improvements in the range of 400 to 600 nm are evident even within just one hour of exposure.

## 6. Preparation of a first prototype for a sampling calorimeter module

Plates with the light output above 300 phe/MeV have been selected for assembling the prototype of a sampling calorimeter module to investigate the principal capabilities for application in medium- and high-energy physics experiments. Two prototypes are composed of scintillator plates of 17x20x5 mm$^3$ in size with all surfaces polished. They are sandwiched between 1 mm thick Pb sheets. The Pb sheets are separated from the scintillator plates by TYVEK paper acting as reflector. The scintillation light is collected along the full sandwiched structure via either a single stripe of green wavelength shifter (WLS, Eljen: EJ-280-10, 20x200x3.0 mm$^3$) or two stripes (20x200x1.5 mm$^3$)

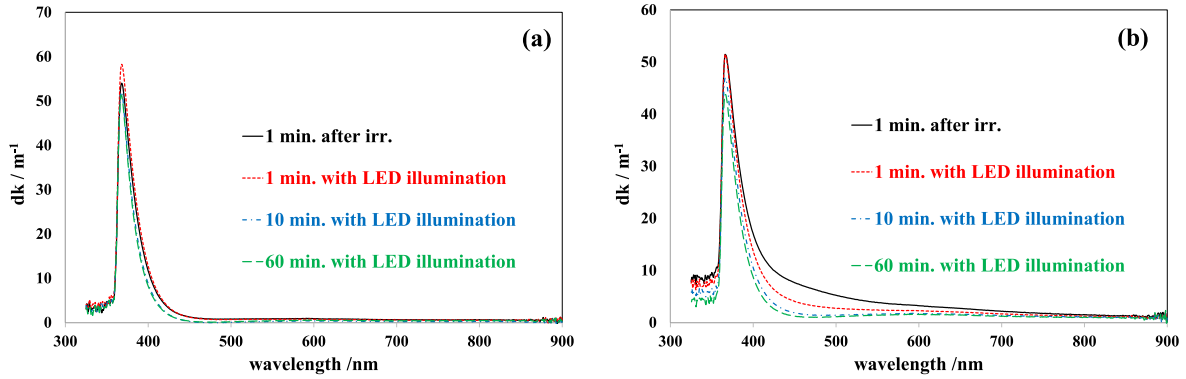


**Fig. 15.** Spectra of radiation-induced absorption coefficient at different durations (indicated) of exposure to external light source emitting at 464 nm in samples with relatively low (a) and high (b) light yield. The measurements were performed at room temperature.

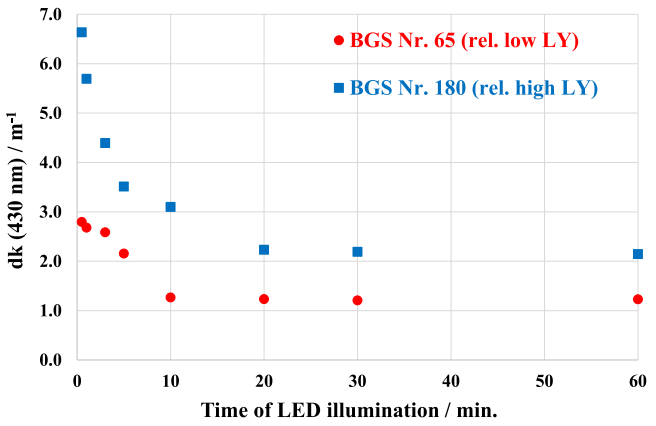


**Fig. 16.** Radiation-induced absorption coefficient at 430 nm as a function of duration of exposure to illumination by a blue light emitting diode (LED) for two selected samples after accumulating the integral $\gamma$-ray irradiation dose of 1000 Gy.. (For interpretation of the references to color in this figure legend, the reader is referred to the web version of this article.)

at two opposite sides. The WLS stripes are directly glued to the BGS plates using optical epoxy glue. The entire detector assembly is covered by Teflon tape and wrapped by a light-tight shrinking tube. Fig. 17 shows assemblies before removing excess glue and wrapping with reflector foil. The black PVC-block at the rear end keeps the extended WLS sheets in place and allows one to attach the PC-board containing photosensors and a preamplifier.

The wavelength-shifted scintillation light is read out with a set of 4 silicon photomultipliers (SiPM KETEK 3325-WB-D0, 3x3 $mm^2$, 25 μm) for each WLS-sheet and amplified in a 1-stage pre-amplifier.

## 7. Neutron detection

Fig. 18 shows the response of the BGS detector to neutrons and to $\gamma$-quanta from different sources to calibrate the energy scale. The relatively low light yield of BGS glass does not allow resolving low-energy $\gamma$-quanta due to the interaction of neutrons with Gd. Nevertheless, the response has two bumps in the regions peaked at 80 keV and 180 keV, which are typical for Gd-containing scintillation materials under exposure to thermal neutrons.

Though no pronounced peaks are observed in the low-energy spectral region, the direct integration of events after background extraction in the range characteristic for $\gamma$-ray lines from (n, $\gamma$) reactions with gadolinium atoms can be used to estimate the sensitivity to neutrons. Table 1 shows the integrated counts collected at different geometries of the measurements in the energy range of 70–200 keV.

As expected at the neutron cross sections of the natural mixture of Gd isotopes, the material is more sensitive to thermal than fast neutrons. An advantage of the glass is its relatively low density in

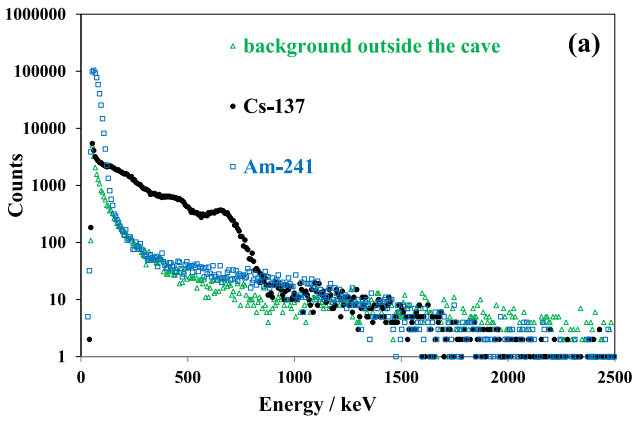


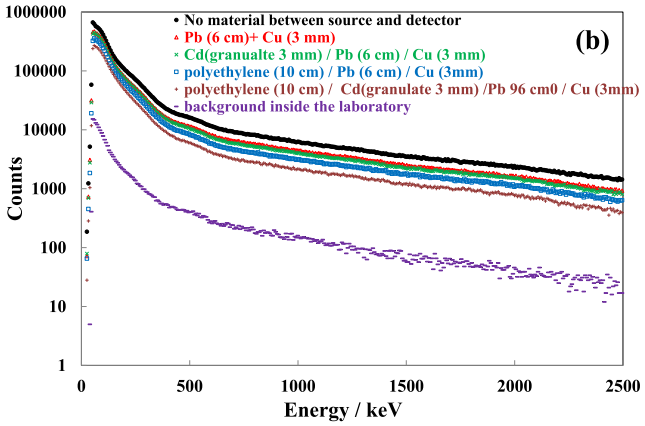


**Fig. 18.** Pulse height spectra measured with BGS glass scintillation detector using $^{241}$Am- and $^{137}$Cs-sources (a) and an Am-Be neutron source with different absorbers placed between the source and detector (b). The measured background is indicated in both measurements.

comparison to Gd-containing single crystals, which makes Ba-Gd silica glass less sensitive to the $\gamma$-background. These results show that the developed glass might be suitable to develop screens for neutron detection.

## 8. Discussion

The developed BGS scintillation glass exhibits an attractive set of scintillation parameters. The properties of the scintillation material achieved to date are summarized in Table 2. The obtained results show that the material can find application in various detectors of $\gamma$-radiation. First of all, we note a good combination of acceptable

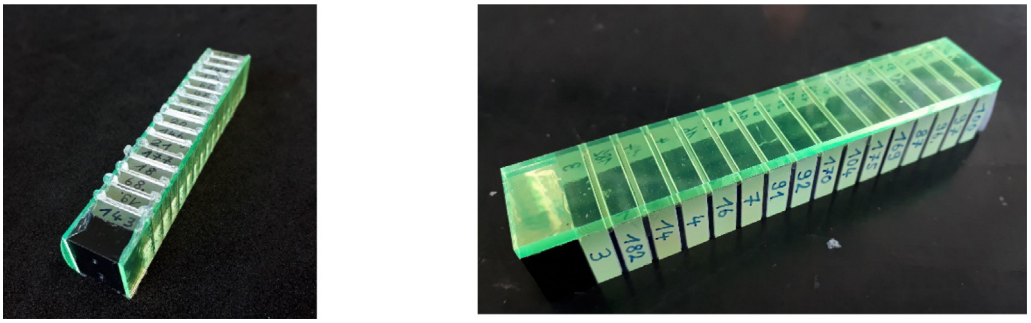

**Fig. 17.** The assembled detector blocks with single and double WLS read out.

**Table 1**
Integrated counts in the energy range 70–200 keV obtained using different absorbers and moderators placed between detector and neutron source. Starting with the second line data are reported after the background subtraction.

| | Measurement geometry | Integrated counts |
|---|---|---|
| 1 | Background in the absence of neutron source | 106 999 |
| 2 | No absorbers or moderators between neutron source and detector | 5 298 225 |
| 3 | Pb/Cu absorbers of $\gamma$-quanta between neutron source and detector | 4 070 277 |
| 4 | Pu/Cu absorbers of $\gamma$-quanta and Cd filter of thermal neutrons between neutron source and detector | 3 911 575 |
| 5 | Response to thermal neutrons (3–4) Pb/Cu – Cd/Pu/Cu | 158 702 |
| 6 | Pb/Cu absorbers of $\gamma$-quanta and polyethylene moderator between neutron source and detector | 3 103 439 |
| 7 | Cd Pu Cu absorbers of $\gamma$-quanta, Cd filter of thermal neutrons and PE moderator between neutron source and detector | 2 363 034 |
| 8 | Response to thermal neutrons with PE moderator (6–7) | 740 405 |

**Table 2**
Properties of scintillation material achieved for the glass with composition specified in the first line.

| | |
|---|---|
| Glass composition, mol % | $SiO_2$-63.0<br>BaO-21.75 $AlF_3$-1.4<br>$Ce_2O_3$-0.76<br>$Gd_2O_3$-13.09 |
| Density, g/cm$^3$ | 4.2 |
| Scintillation emission peak position, nm | 430 |
| Scintillation decay times and weight coefficients, ns (%) | 90 (45%)<br>400 (55%) |
| Coincidence time resolution, ps | 230 ± 65 |
| Light yield within 4 μs gate, ph/MeV | ≤2500 ± 5% |
| Temperature coefficient of light yield, %/°C | 0.3 |
| Attenuation length at emission wavelength, cm | 50 |

scintillation yield and good radiation resistance of the material. Scintillation glass has a good potential for further improvement, though certain technological means extensively used in the production of crystalline scintillation materials, such as co-doping, would hardly be applicable to glass scintillator. The variation in matrix composition is one of the most promising approaches to improve the scintillation properties of glass scintillators. In particular, the further increase in the gadolinium content in the matrix is a key approach to achieve an even better set of the scintillation properties. Firstly, this will decrease the average distance between the Gd subnet ions and, consequently, facilitates faster migration of electronic excitations, mostly Frenkel-type excitons, along the Gd subnet in the glass and will increase the rate of transfer of electronic excitations from gadolinium to the activator. As a result, a significant reduction in the contribution of the slow component with the decay time of ∼400 ns might be expected. Secondly, the increase in the content of heavy ions in the glass will lead to an increase in the probability of photo-absorption of $\gamma$-quanta, which will favorably affect the $\gamma$-quanta detection efficiency.

In spite of its relatively low scintillation yield, the Ce-doped BGS scintillator exhibits a good CTR, which is similar to the values obtained using the same setup for BGO single crystals with a significant higher light yield. In the long run, the development of hybrid detector modules is feasible, since the technology of applying a photosensitive layer is sufficiently well developed for glass substrates.

Last but not least, an important feature is the capability of the Gd-containing glass to detect neutrons. Contrary to Li-glass, which requires enrichment with $^6$Li isotope, the BGS glass utilizes an inexpensive natural mixture of Gd isotopes making the fabrication costs affordable. However, further development to enable the direct identification of neutron triggered events is still needed.

## 9. Conclusion

A new heavy scintillation glass containing Ba, Gd, Ce, and Si ions and exhibiting a light yield of ∼2500 ph/MeV has been developed. A similar light yield was achieved at two production facilities. The light yield shows only a negligible temperature dependence in the range from −40 °C to +20 °C, good tolerance to ionizing radiation, and two components of the scintillation decay with characteristic times of 90 ns and 400 ns. The further development of the Ce-doped BGS glass scintillator should be focused on the reduction of the contribution of slow decay component, casting of highly homogeneous large-volume blocks, as well as on a better control of the relative content of $Ce^{4+}$ ions to avoid coloring of the material.

## CRediT authorship contribution statement

**V. Dormenev:** Validation, Formal analysis, Investigation, Resources, Data curation, Writing – original draft, Writing – review & editing, Visualization, Conceptualization. **A. Amelina:** Investigation. **E. Auffray:** Conceptualization, Data curation, Validation, Writing – original draft, Writing – review & editing. **K.-T. Brinkmann:** Conceptualization, Project administration, Resources, Writing – original draft. **G. Dosovitskiy:** Investigation, Resources, Data curation, Writing – original draft, Writing – review & editing. **F. Cova:** Validation, Formal analysis, Investigation, Data curation, Writing – original draft, Writing – review & editing, Visualization, Conceptualization. **A. Fedorov:** Formal analysis, Investigation. **S. Gundacker:** Methodology, Validation, Formal analysis, Investigation, Writing – original draft. **D. Kazlou:** Formal analysis, Investigation, Resources, Data curation. **M. Korjik:** Conceptualization, Validation, Writing – original draft, Writing – review & editing. **N. Kratochwil:** Validation, Formal analysis, Investigation, Data curation, Writing – original draft, Writing – review & editing, Visualization, Methodology. **V. Ladygin:** Validation, Resources, Data curation. **V. Mechinsky:** Validation, Formal analysis, Investigation. **M. Moritz:** Validation, Writing – original draft, Formal analysis. **S. Nargelas:** Validation, Formal analysis, Investigation, Data curation, Visualization. **R.W. Novotny:** Writing – original draft, Writing – review & editing, Visualization, Conceptualization. **P. Orsich:** Validation, Formal analysis, Investigation. **M. Salomoni:** Validation, Formal analysis, Investigation. **Y. Talochka:** Validation, Formal analysis, Investigation, Data curation. **G. Tamulaitis:** Conceptualization,

Data curation, Writing – original draft, Writing – review & editing, Visualization. **A. Vaitkevicius:** Validation, Formal analysis, Investigation, Data curation. **A. Vedda:** Conceptualization, Writing – original draft, Writing – review & editing, Visualization, Data curation. **H.-G. Zaunick:** Project administration, Resources, Validation, Data curation.

## Declaration of competing interest

The authors declare that they have no known competing financial interests or personal relationships that could have appeared to influence the work reported in this paper.

## Acknowledgments

This work was carried out in the framework of Crystal Clear Collaboration. We thank for supporting funding from the European Union Horizon 2020 Research and Innovation Programmes under Grant Agreement no. 777222 (ATTRACT) and No 654002 (INTELUM). We thank S. Polma and Team from PRECIOSA for contribution in glass technology development and effective management of sample production. Authors (b, c, h) are grateful for support of the Government of the Russian Federation (grant no. 14.W03.31.0004), and the JINR- INP BSU, Russia contract No 100-2673.

## References

[1] P. Lecoq, A. Gektin, M. Korzhik, Inorganic Scintillators for Detector Systems, Springer, 2017.

[2] F. Cova, M. Fasoli, F. Moretti, N. Chiodini, K. Pauwels, E. Auffray, M.T. Lucchini, E. Bourret, I. Veronese, E. d'Ippolito, A. Vedda, Optical properties and radiation hardness of Pr-doped Sol-Gel silica: influence of fiber drawing process, J. Lumin. 192 (2017) 661–667.

[3] F. Cova, F. Moretti, M. Fasoli, N. Chiodini, K. Pauwles, E. Auffray, M. Toliman Lucchini, S. Baccaro, A. Cemmi, H. Bartova, A. Vedda, Radiation hardness of Ce-doped sol–gel silica fibers for high energy physics applications, Opt. Lett. 43 (4) (2018) 903–906.

[4] F. Cova, M.T. Lucchini, K. Pauwels, E. Auffray, N. Chiodini, M. Fasoli, A. Vedda, Dual cherenkov and scintillation response to high-energy electrons of rare-earth doped silica fibers, Phys. Rev. Appl. 11 (2019) 024036.

[5] A.R. Spowart, Neutron scintillating glasses: part II. The effect of temperature on pulse height and conductivity, Nucl. Instrum. Methods Phys. Res. 140 (1977) 19–28.

[6] A.R. Spowart, Neutron scintillating glasses: part III. Pulse decay time measurements at room temperature, Nucl. Instrum. Methods Phys. Res. 150 (1978) 159–163.

[7] Y. Tratsiak, A. Fedorov, G. Dosovitsky, O. Akimova, E. Gordienko, M. Korjik, V. Mechinsky, E. Trusova, Scintillation efficiency of binary $Li_2O$-$2SiO_2$ glass doped with $Ce^{3+}$ and $Tb^{3+}$ ions, J. Alloys Compd. 735 (2018) 2219–2224.

[8] A. Borisevich, V. Dormenev, M. Korjik, D. Kozlov, V. Mechinsky, R.W. Novotny, Optical transmission radiation damage and recovery stimulation of DSB:$Ce^{3+}$ inorganic scintillation material, J. Phys. Conf. Ser. 587 (2015) 012063.

[9] M.V. Korjik, A. Vaitkevicius, D. Dobrovolskas, E.V. Tret'yak, E. Trusova, G. Tamulaitis, Distribution of luminescent centers in $Ce^{3+}$-ion doped amorphous stoichiometric glass BaO-$2SiO_2$ and dedicated glass ceramics, Opt. Mater. 47 (2015) 129–134.

[10] E. Auffray, N. Akchurin, A. Benaglia, A. Borisevich, C. Cowden, J. Damgov, V. Dormenev, C. Dragoiu, P. Dudero, M. Korjik, D. Kozlov, S. Kunori, P. Lecoq, S.W. Lee, M. Lucchini, V. Mechinsky, K. Pauwels, DSB: $Ce^{3+}$ scintillation glass for future, J. Phys. Conf. Ser. 587 (2015) 012062.

[11] K.-T. Brinkmann, A. Borisevich, S. Diehl, V. Dormenev, J. Houzvicka, M. Korjik, R.W. Novotny, H.-G. Zaunick, S. Zimmermann, Research activity with different types of scintillation materials, J. Phys. Conf. Ser. 763 (2016) 012002.

[12] R.W. Novotny, D. Bremer, V. Dormenev, W. Döring, T. Eissner, M. Korzhik, T. Kuske, O. Missevitch, M. Moritz, The PANDA electromagnetic calorimeter—A high-resolution detector based on PWO-II, IEEE Trans. Nucl. Sci. 57 (3 part 2) (2010) 1441–1446.

[13] E. Auffray, K.-T. Brinkmann, F. Cova, S. Gundacker, N. Kratochwil, M. Moritz, S. Nargelas, R.-W. Novotny, P. Orsich, G. Tamulaitis, A. Vaitkevicius, A. Vedda, H.-G. Zaunick, Development of radiation-hard and cost-effective inorganic scintillators for calorimetric detectors based on binary glass compositions doped with cerium – SCINTIGLASS, 2021, available at https://attract-eu.com/wp-content/uploads/2019/05/SCINTIGLASS.pdf. (Accessed 5 January 2021).

[14] G. Tamulaitis, A. Vasil'ev, M. Korzhik, A. Mazzi, A. Gola, S. Nargelas, A. Vaitkevičius, A. Fedorov, D. Kozlov, Improvement of the time resolution of radiation detectors based on $Gd_3Al_2Ga_3O_{12}$ scintillators with SiPM readout, IEEE Trans. Nucl. Sci. 66 (2019) 1879–1888.

[15] Attract featured stories: Development of radiation-hard and cost–effective inorganic scintillators for calorimetric detectors based on binary glass compositions doped with cerium (SCINTIGLASS), 2021, available at https://attract-eu.com/attract-featured-stories-scintiglass/. (Accessed 4 January 2021).

[16] R.W. Novotny, K.-T. Brinkmann, A. Borisevich, V. Dormenev, M. Korjik, D. Kozlov, P. Orsich, H.-G. Zaunick, S. Zimmermann, Study of the Glass and Glass Ceramic Stoichiometric and $Gd^{3+}$ Heavy Loaded BaO*$2SiO_2$: Ce (DSB: Ce) Scintillation Materials for Calorimetry Application, in: Conference Record IEEE NSS MIC, San Diego, CA, United States, 2015, N3D1-3.

[17] R.W. Novotny, K.-T. Brinkmann, A. Borisevich, V. Dormenev, M. Korjik, H.-G. Zaunick, S. Zimmermann, Study of the new glass and glass ceramic stoichiometric and $Gd^{3+}$-loaded BaO*$2SiO_2$ (DSB: Ce) scintillation material for future calorimetry, J. Phys. Conf. Ser. 928 (2017) 012034.

[18] R.W. Novotny, K.-T. Brinkmann, V. Dormenev, P. Drexler, M. Korjik, D. Kozlov, H.-G. Zaunick, Performance of DSB – a new glass and glass ceramic as scintillation material for future calorimetry, J. Phys. Conf. Ser. 1162 (2019) 012023.

[19] V.M. Abazov, et al., The SPD proto Collaboration, Conceptual design of the spin physics detector, 2021, available at https://arxiv.org/abs/2102.00442. (Accessed 15 May 2021).

[20] A.Z. Schwarzchild, E.K. Warbuston, The measurement of short nuclear lifetimes, Ann. Rev. Nucl. Part. Sci. 18 (1968) 265–290.

[21] L.M. Bollinger, G.E. Thomas, Measurement of the time dependence of scintillation intensity by a delayed-coincidence method, Rev. Sci. Instrum. 32 (9) (1961) 1044–1050.

[22] S. Gundacker, R.M. Turtos, N. Kratochwil, R.H. Pots, M. Paganoni, P. Lecoq, E. Auffray, Experimental time resolution limits of modern SiPMs and TOF-PET detectors exploring different scintillators and Cherenkov emission, Phys. Med. Biol. 65 (2020) 025001.

[23] S. Gundacker, R.M. Turtos, E. Auffray, M. Paganoni, P. Lecoq, High-frequency SiPM readout advances measured coincidence time resolution limits in TOF-PET, Phys. Med. Biol. 64 (2019) 055012.

[24] M. Korzhik, G. Tamulaitis, A. Vasil'ev, Physics of Fast Processes in Scintillators, Springer, 2020, p. 250.

[25] Y. Tratsiak, M. Korzhik, A. Fedorov, G. Dosovitsky, O. Akimova, S. Belus, M. Fasoli, A. Vedda, V. Mechinsky, E. Trusova, On the stabilization of Ce, Tb, and Eu ions with different oxidation states in silica-based glasses, J. Alloys Compd. 797 (2019) 302–308.

[26] Y. Tratsiak, M. Korjik, A. Fedorov, G. Dosovitsky, O. Akimova, E. Gordienko, M. Fasoli, V. Mechinsky, A. Vedda, F. Moretti, E. Trusova, Luminescent properties of binary MO-$2SiO_2$ (M = $ca^{2+}$, $Sr^{2+}$, $Ba^{2+}$) glasses doped with $Ce^{3+}$, $Tb^{3+}$ and $Dy^{3+}$, J. Alloys Compd. 765 (2018) 207–212.

[27] N. Kratochwil, S. Gundacker, P. Lecoq, E. Auffray, Pushing Cherenkov PET with BGO via coincidence time resolution classification and correction, Phys. Med. Biol. 65 (11) (2020) 115004.

[28] A. Borisevich, V. Dormenev, A. Fedorov, M. Korjik, T. Kuske, V. Mechinsky, O. Missevitch, R. Novotny, R. Rusack, A. Singovsky, Stimulation of radiation damage recovery of lead tungstate scintillation crystals operating in a high dose-rate radiation environment, IEEE Trans. Nucl. Sci. 60 (2 part 2) (2013) 1368–1372.

[29] P. Orsich, V. Dormenev, K.-T. Brinkmann, M. Korjik, M. Moritz, R.-W. Novotny, H.-G. Zaunick, Stimulated recovery of the radiation damage in lead tungstate crystals, IEEE Trans. Nucl. Sci. 67 (6) (2020) 952–955.